Simple models for wet-snow accretion on transmission lines: snow load and liquid water content

G. Poots and P. L. I. Skelton
Centre for Industrial Applied Mathematics, University of Hull, Hull, UK

A simplified heat and mass transfer model is proposed for wet-snow accretion on an overhead transmission line conductor. The accretion processes near the tower and the center of the span are formulated using the large relaxation time approximation (LRTA) and the cylindrical-sleeve approximation (CSA), respectively. The heat and mass transfer equations governing the snow evolution process are solved analytically to yield predictions for the snow load and the liquid water content of the snow matrix as a function of the wind speed, relative humidity, air temperature, precipitation rate, and diameter and thermal properties of the conductor. The interactive roles of these meteorological and physical variables are analyzed for the one-dimensional problems of snow accretion in a plane layer and cylindrical-sleeve growth on a conductor, and for the two-dimensional problem of snow accretion by axial growth. Effects due to wet-snow densification and the accretion factor for snowflake impaction are also incorporated.

Keywords: overhead power conductors; wet snow

Introduction

General

Wet-snow accretion occurs on overhead line conductors in the air-temperature range $T_a \in [0, 5]$°C. In the accretion process, a snowflake, which is a mixture of air, ice, and water, collides with the snow/conductor surface and suffers fragmentation. It is observed (see Wakahama et al. 1977) that some of the fragments adhere to the surface and the remainder ricochet into the air flow. During the accretion process, the wet snow undergoes a rapid process of metamorphosis in which the snow fragments form a snow matrix held together by capillary forces and ice bonding. The strength of these forces depends on the liquid water content (LWC) of the snow matrix: if the LWC is greater than 40% (see Admirat et al. 1988a), the wet-snow adhesion is greatly reduced, and the snow deposit is shed due to wind force and aerodynamic torque. Hence, the problem of the prediction of wet-snow load, relevant to design criteria for overhead line conductors, is allied to the study of the thermodynamic state of the snow deposit.

In this paper, existing theoretical snow models for the prediction of snow load on a conductor are reviewed, and a thermodynamic model for the prediction of the LWC of the snow matrix is extended. Two limiting modes of snow accretion, which occur on the conductor span, are examined. It is the aim of this paper to predict the LWC of these modes during the snow evolution process.

Address reprint requests to Professor Poots at the Centre for Industrial Applied Mathematics, University of Hull, Hull, HU6 7RX, UK.

Received 19 November 1993; accepted 21 April 1994

Wet-snow load

The calculation of the snow load on a conductor of finite span and finite torsional stiffness is described in Skelton and Poots (1991); here it was assumed that all of the snow adheres on impact, so that the snow accretion factor is unity. A feature of this mathematical model is that snowflakes, because of their inertia, follow rectilinear paths in the wind direction prior to impaction. At the towers, where the conductor is anchored, axial growth on the windward side is observed (see Figure 1a). A consequence of this eccentric snow load is that the conductor rotates, and the degree of rotation is further enhanced by the effect of aerodynamic moment. Consequently, there is a progressive development of cylindrical-sleeve growth at midspan (see Figure 1b).

These two modes of wet-snow evolution are adequately represented by approximate snow models. Thus, axial growth is given by the large relaxation time approximation (LRTA) of Poots and Rodgers (1976) and cylindrical-sleeve growth by the cylindrical-sleeve approximation (CSA) as reported in Admirat

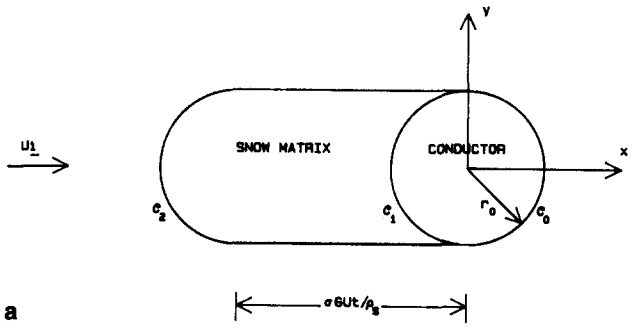

a

Figure 1a Schematic diagram of LRTA snow accretion on a conductor

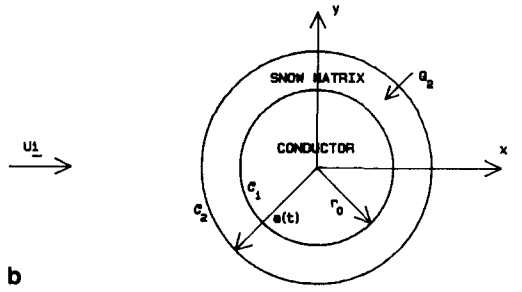

Figure 1b Schematic diagram of CSA snow accretion on a conductor

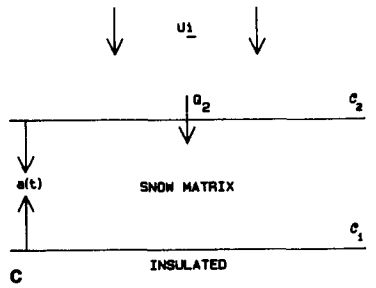

Figure 1c One-dimensional thermodynamic wet-snow model

and Sakamoto (1988). In the following, it is assumed that the meteorological conditions and the accretion factor remain constant during the snowstorm.

For axial growth, the LRTA is based on the mass transfer balance

$$dM/dt = \sigma GU2r_0, \quad M(0) = 0 \tag{1}$$

Here $G(\text{kg.m}^{-3}) = P/(3600 \times V_T)$ is the liquid water content of the air and $V_T(\text{m.s}^{-1})$ is the snowflake terminal speed corresponding to the precipitation rate $P(\text{mm}(H_2O).\text{h}^{-1})$; $U(\text{m.s}^{-1})$ is the wind speed, and $2r_0(\text{m})$ is the diameter of the conductor. For steady environmental conditions,

$$M(t) = 2\sigma GUr_0 t \tag{2}$$

and the shape of the axial growth, as given by Poots and Rodgers (1976), on solving a snow evolution equation is

$$(x + \sigma GUt/\rho_s)^2 + y^2 = r_0^2 \tag{3}$$

(see Figure 1a); $\rho_s(\text{kg.m}^{-3})$ is the density of the accreted snow.

For cylindrical-sleeve growth, the CSA is governed by the mass transfer balance

$$dM/dt = \sigma GU2a(t), \quad M(0) = 0 \tag{4}$$

where $a(t)$ is the radius of the snow sleeve. Moreover, the mass of snow accreted at any time is given by

$$M(t) = \pi\rho_s(a(t)^2 - r_0^2) \tag{5}$$

(see Figure 1b). For steady environmental conditions, Equations 4 and 5 yield the solution

$$M(t) = 2\sigma GUtr_0 + (\sigma GUt)^2/\pi\rho_s \tag{6}$$

$$a(t) = \sigma GUt/\pi\rho_s + r_0 \tag{7}$$

In general, the accretion factor σ, the snow density ρ_s, and the liquid water content of a snowflake γ (prior to impaction) are functions of the meteorological data (T_a, P, U), the relative humidity Hr, and the physical constants of the conductor system. For a specified geographic environment, these parameters can be obtained on validation of the CSA model using field measurements. Thus σ and ρ_s are deduced on ensuring that the theoretical snow load, given by Equation 6, is coincident with field measurements. For France, Admirat et al. (1988b) suggest

$$\sigma = 0.88/U^{0.88}, \quad \rho_s = 100 + 20U, \quad \gamma = 0.04T_a^2, \tag{8}$$

and it is assumed that this parameterization is relevant to wet-snow episodes in the UK. In particular, snow densification is seen to be proportional to the wind speed, and the accretion factor is roughly in the range 0.1 to 0.2 for wind speeds $U \in [5, 10](\text{m.s}^{-1})$. Further information on the parameterization of σ and ρ_s is available from wind tunnel experiments by Sakamoto et al. (1986). Here, on validation of the CSA model (Equations 6 and 7), wet-snow data is given for σ and ρ_s as a function of T_a, P, U, and r_0. The accretion factor σ is shown to depend on the air temperature T_a, as well as U, and appears

Notation

a	Radial thickness of cylindrical snow sleeve, m
Bi	Biot number
c_a	Specific heat of air, $\text{J.kg}^{-1}\,\text{K}^{-1}$
e_i	Saturation vapor pressure over ice, kPa
e_w	Saturation vapor pressure over water, kPa
G	Liquid water content per unit volume of air, kg.m^{-3}
$\bar{h}$	Average heat transfer coefficient, $\text{W.m}^{-2}\,\text{K}^{-1}$
H_0	Atmospheric pressure, kPa
Hr	Relative humidity
K_a	Thermal conductivity of air, $\text{W.m}^{-1}\,\text{K}^{-1}$
K_0	Thermal conductivity of conductor, $\text{W.m}^{-1}\,\text{K}^{-1}$
L_E	Latent heat of evaporation, J.kg^{-1}
L_f	Latent heat of fusion, J.kg^{-1}
L_S	Latent heat of sublimation, J.kg^{-1}
M	Snow load per unit length, kg.m^{-1}
M_w	Mass of water in snow matrix, kg.m^{-1}
Nu	Nusselt number
P	Snow precipitation rate, mm $(H_2O).\text{h}^{-1}$
Q	Heat flux, W.m^{-2}
r	Radial coordinate, m
R	Dimensionless radial polar coordinate
Re	Reynolds number for conductor
r_0	Radius of conductor, m
t	Time, s
T	Dimensionless time
T_a	Ambient air temperature, °C
T_f	Fusion temperature, °C
T_0	Conductor temperature, °C
U	Wind speed, m.s^{-1}
V_T	Terminal velocity of average-sized snowflake, m.s^{-1}
(x, y)	Cartesian coordinates, m

Greek symbols

γ	Liquid water content of snowflake
η_a	Viscosity of air, N.sm^{-2}
θ	Angular polar coordinate
Θ	Dimensionless temperature of conductor
Λ	Liquid water content of snow matrix
ν_a	Kinematic viscosity of air, $\text{m}^2.\text{s}^{-1}$
ρ_s	Density of snow matrix, kg.m^{-3}
σ	Accretion factor
χ_i	Heat transfer parameter for ice
χ_w	Heat transfer parameter for water

to attain maximum values when $T_a \approx 2°C$. Furthermore, in these wind tunnel simulations, values of $\sigma \in [0.1, 1]$ were recorded.

In the development of thermodynamic models for the prediction of LWC in axial and cylindrical-sleeve growth, it is assumed that densification depends linearly on U, as in Equation 8, and that σ satisfies the inequality

$$V_T/U < \sigma(U) \leq 1 \tag{9}$$

This inequality is established using the following argument. The mass transfer rate for freely falling snow, across a surface, is

$$(\dot{M}_s'')_T = GV_T(\text{kg.m}^{-2}\text{s}^{-1}) \tag{10}$$

and the mass transfer for the driven snow is

$$(\dot{M}_s'') = \sigma GU(\text{kg.m}^{-2}\text{s}^{-1}) \tag{11}$$

Since more snow is expected to adhere during a wind-driven accretion process than during the accretion of freely falling snow, it follows that

$$(\dot{M}_s'') > (\dot{M}_s'')_T \tag{12}$$

and hence

$$\sigma > V_T/U \tag{13}$$

For zero wind ($U = 0$, $V_T \approx 1\text{m.s}^{-1}$), $\sigma \leq 1$, and hence the inequality is as stated in Equation 9. It is of interest to note that the lower limit for σ is almost identical to the value recommended by Admirat et al. (1988b) (see Equation 8; also Admirat et al. (1988b) suggest the use of $\sigma = 1/U$ for France and Japan).

For the two modes of wet-snow accretion, the snow load is computed using the LRTA and CSA models (Equations 2 and 6, respectively). In the next section, the related time-dependent models are developed for calculating the LWC of the snow matrix during the snow evolution process. Results are given for the extreme values of the accretion factor, namely, $\sigma = V_T/U$ and $\sigma = 1$.

Thermodynamic models for the prediction of liquid water content of the snow matrix

The growth and shedding of wet snow on overhead line conductors is controlled by both thermal and wind effects. Ignoring the latter, Grenier et al. (1986) formulated a thermodynamical model for wet-snow accretion in the form of a cylindrical sleeve. On consideration of the thermal interaction of the wet-snow sleeve with the environment, a snow surface heat balance gave details of the LWC of the snow sleeve in positive air temperatures; consideration, from the viewpoint of wet-snow shedding, was also given to the increase of LWC by means of Joule heating.

The basic approach of Grenier et al. (1986) is now employed to formulate the LWC models for the two limiting modes of accretion, namely, axial and cylindrical-sleeve growth. Firstly, however, consideration is given to the simple one-dimensional (1-D) thermodynamic model of snow growth and LWC due to snowflakes impacting in a perpendicular direction to a plane wall; the model relates to snowflake impaction in the neighborhood of the stagnation line in the flow past a bluff body. This consideration is followed by the related 1-D model for CSA growth, as studied earlier by Grenier et al. (1986), and by two-dimensional (2-D) models for axial growth.

The one-dimensional plane snow layer

Let the thickness of the wet-snow layer attached to the thermally insulated plane surface $\mathscr{C}_1$ be $a(t)$ and let snowflakes impact on the wet-snow/air interface $\mathscr{C}_2$ with speed U (see Figure 1c). The mass balance at $\mathscr{C}_2$ gives

$$\rho_s \frac{da}{dt} = \sigma GU,\ a(0) = 0 \tag{14}$$

and for steady-state environmental conditions

$$a(t) = \sigma GUt/\rho_s. \tag{15}$$

The energy balance at $\mathscr{C}_2$ consists of the heat gained by convection and the heat lost by evaporation and sublimation. The convective heat transfer between the ambient air and the snow layer, which has temperature T_f throughout, is

$$Q_2^a = \bar{h}(T_a - T_f) \tag{16}$$

where $T_f(°C)$ is the fusion temperature and h ($\text{W.m}^{-1}\,\text{K}^{-1}$) is the surface heat transfer coefficient. Heat transfer to the air by evaporation from a *water surface* is

$$Q_2^w = \chi_w[e_w(T_a) - e_w(T_f)] = \chi_w \Delta e_w \tag{17}$$

and by sublimation from an *ice surface* is

$$Q_2^i = \chi_i[e_i(T_a) - e_i(T_f)] = \chi_i \Delta e_i \tag{18}$$

where $e(T)$(kPa) is the saturation vapor pressure at temperature T. Polynomial expressions for calculating saturation pressure over ice and over water are available in Lowe (1977). Furthermore, application of the heat and mass transfer analogy of Chilton and Colburn (1934) yields

$$\chi_w = 0.622\bar{h}L_E\text{Hr}/(c_aH_0l^{2/3}),\ \chi_i = 0.622\bar{h}L_S\text{Hr}/(c_aH_0l^{2/3}) \tag{19}$$

where $L_E(\text{J.kg}^{-1})$ and $L_S(\text{J.kg}^{-1})$ are the latent heat of evaporation and sublimation, respectively, $c_a(\text{J.kg}^{-1}\,\text{K}^{-1})$ is the specific heat of air, H_0(kPa) is the air pressure, and $l = 0.875$ is the Lewis number. The LWC of the snow matrix, denoted by Λ, is defined as the ratio of the mass of liquid to the total mass of liquid and ice per unit volume. It is further assumed that the surface $\mathscr{C}_2$ has composition in the ratio of Λ for water to $(1 - \Lambda)$ for ice, i.e., partitioned in the same way as for the snow matrix. On neglecting heat gained by radiation, the heat flux at $\mathscr{C}_2$ is

$$Q_2 = Q_2^a - \Lambda Q_2^w - (1 - \Lambda)Q_2^i \tag{20}$$

$$= \bar{h}(T_a - T_f) - \Lambda\chi_w\Delta e_w - (1 - \Lambda)\chi_i\Delta e_i \tag{21}$$

and the rate of production of melt water within the snow matrix is

$$L_f \frac{dM_w}{dt} = Q_2,\ M_w(0) = 0 \tag{22}$$

The liquid water content is thus given by the ratio

$$\Lambda = \frac{\gamma\sigma GUt + Q_2 t/L_f}{\sigma GUt} \tag{23}$$

yielding the expression

$$\Lambda = \frac{(\gamma + \delta)}{(1 - \varepsilon)}, \tag{24}$$

where the constant parameters

$$\delta = [\bar{h}(T_a - T_f) - \chi_i\Delta e_i]/\sigma GUL_f, \tag{25}$$

$$\varepsilon = -[\chi_w\Delta e_w - \chi_i\Delta e_i]/\sigma GUL_f > 0, \tag{26}$$

and $\varepsilon \ll 1$. The important result here is that within the evolving snow layer, the LWC is independent of time and is proportional to the heat transfer ratio $\bar{h}(T_a - T_f)/(\sigma GUL_f)$.

The one-dimensional cylindrical sleeve

The snow load and snow-sleeve thickness for this model are given by Equations 6 and 7 (see Figure 1b). To formulate the energy balance at the snow surface, it is necessary to specify the heat transfer coefficient for the snow sleeve in a cross flow of air. Apart from adopting an average heat transfer coefficient for a bare circular cylinder as in Poots and Skelton (1992), the only available heat transfer data relevant to snow cylinders is that obtained by Szilder et al. (1988). Average heat transfer coefficients

$$\bar{h} = \overline{\mathrm{Nu}} K_a / 2r_0 \tag{27}$$

were measured for four typical ice-accretion shapes. The length scale for the accretion was taken to be the diameter of the bare conductor, $2r_0$; recommended values of the average Nusselt number, $\overline{\mathrm{Nu}}$, are given as

$$\overline{\mathrm{Nu}} = 0.117\mathrm{Re}^{0.68} \tag{28}$$

for the Reynolds number range $\mathrm{Re} \in [1.5 \times 10^4, 1.7 \times 10^5]$. In the above, $K_a(\mathrm{W.m^{-1}\,K^{-1}})$ is the thermal conductivity of air, and the Reynolds number, based on the diameter $2r_0(\mathrm{m})$, is

$$\mathrm{Re} = 2r_0 U / \nu_a \tag{29}$$

where $\nu_a(\mathrm{m^2.s^{-1}})$ is the kinematic viscosity of air.

The total heat flux across $\mathscr{C}_2$ into the snow sleeve is

$$\bar{Q}_2 = 2\pi a(t) Q_2 \tag{30}$$

where the local heat flux Q_2 is expressed as

$$Q_2 = \bar{h}(T_a - T_f) - \Lambda\chi_w \Delta e_w - (1 - \Lambda)\chi_i \Delta e_i \tag{31}$$

(see Equation 21). The rate of melting of the ice within the snow matrix is given by

$$L_f \frac{dM_w}{dt} = \bar{Q}_2 \tag{32}$$

and hence

$$\Lambda(t) = \frac{\int_0^t \gamma\sigma G U 2a(t)dt + \int_0^t (\bar{Q}_2/L_f)dt}{\pi\rho_s(a^2(t) - r_0^2)} \tag{33}$$

For convenience, introduce the new dimensionless time variable

$$T = \sigma G U t / \rho_s r_0 \tag{34}$$

Then the snow load and snow-sleeve thickness, from Equations 6 and 7, transform to

$$M(t) = \pi\rho_s(a^2 - r_0^2) = \rho_s r_0^2 (2T + T^2/\pi) \tag{35}$$

$$a(T) = r_0(1 + T/\pi) \tag{36}$$

respectively. In terms of this variable, the LWC becomes

$$\Lambda(T) = \gamma + \frac{\int_0^T (1 + T/\pi) Q_2 dT}{(T + T^2/2\pi)(\sigma G U L_f)} \tag{37}$$

$$= \gamma + \frac{\pi\delta\int_0^T (1 + T/\pi)dT + \pi\varepsilon\int_0^T (1 + T/\pi)\Lambda dT}{(T + T^2/2\pi)} \tag{38}$$

Consequently, the first-order differential equation for $\Lambda(T)$ is

$$\frac{d\Lambda}{dT} + \Lambda(1 - \pi\varepsilon)\frac{(1 + T/\pi)}{(T + T^2/2\pi)} = (\gamma + \pi\delta)\frac{(1 + T/\pi)}{(T + T^2/2\pi)} \tag{39}$$

Although the general solution of this equation is singular, it possesses the required *nonsingular* solution

$$\Lambda = \frac{\gamma + \pi\delta}{1 - \pi\varepsilon} \tag{40}$$

As in the previous 1-D solution (Equation 24), the LWC for the 1-D cylindrical-sleeve growth, given by Equation 40, is also independent of time and is proportional to $\bar{h}(T_a - T_f)/(\sigma G U L_f)$. It is not, however, inversely proportional to the snow-sleeve diameter as reported in Grenier et al. (1986).

The two-dimensional axial growth

The snow load and LRTA profile for axial growth are given in Equations 2 and 3, respectively (see Figure 1a). In terms of the dimensionless time T, the snow load is

$$M(T) = 2\rho_s r_0^2 T \tag{41}$$

The global change in the LWC of the snow matrix is due to convective, evaporative, and sublimative heat transfer across the snow surface, $\mathscr{C}_2$, and heat transfer by conduction across the conductor to the root of the snow deposit, $\mathscr{C}_1$. Consider the thermodynamic model for LWC in the case when the conductor surface is *insulated*, i.e., there is no heat transfer from the environment through $\mathscr{C}_1$. The rate of production of melt water within the snow matrix is given by

$$L_f \frac{dM_w}{dt} = (2\sigma G U t/\rho_s + \pi r_0) \times [\bar{h}(T_a - T_f) - \Lambda\chi_w \Delta e_w - (1 - \Lambda)\chi_i \Delta e_i] \tag{42}$$

which, in dimensionless variables, is

$$\frac{d}{dT}\left(\frac{M_w}{\rho_s r_0^2}\right) = 2\left(T + \frac{\pi}{2}\right)(\delta + \varepsilon\Lambda) \tag{43}$$

Therefore, the LWC is governed by the equation

$$\Lambda(T) = \gamma + \frac{1}{T}\int_0^T \left(T + \frac{\pi}{2}\right)(\delta + \varepsilon\Lambda)dT \tag{44}$$

yielding the first-order differential equation

$$\frac{d\Lambda}{dT} + \Lambda\frac{1}{T}\left(1 - \frac{\pi}{2}\varepsilon - \varepsilon T\right) = \frac{1}{T}\left(\gamma + \frac{\pi}{2}\delta + \delta T\right) \tag{45}$$

The solution to this equation is given by

$$\Lambda(T) = \frac{\gamma^*}{1 - \pi\varepsilon/2} + \left(\frac{\gamma^*\varepsilon}{1 - \pi\varepsilon/2} + \delta\right) T \exp(\varepsilon T) \sum_{r=0}^{\infty} \frac{(-1)^r(\varepsilon T)^r}{(2 - \pi\varepsilon/2 + r)r!} \tag{46}$$

where the series is convergent for all values of εT. In the *insulated* case, γ^* is defined as

$$\gamma^* = \gamma + \pi\delta/2 \tag{47}$$

Thus for the 2-D axial growth mode, with snow root insulated, the LWC is a function of the time.

Consider now the thermodynamic model for the LWC in the more realistic case, when the snow root gains heat from the environment by conduction across $\mathscr{C}_1$, i.e., the conductor is *not insulated*. The thermal state of the conductor is controlled by the isothermal surface temperature $T_0 = T_f$ at the snow/conductor surface $\mathscr{C}_1$ and by the convective heating on the bare surface $\mathscr{C}_0$ due to the wind. During the snow accretion process, assume a steady-state temperature within the

conductor: this entails solving the heat conduction problem

$$\nabla^2 T_0 = 0, r \le r_0 \tag{48}$$

$$T_0 = T_f \text{ on } \mathscr{C}_1 \tag{49}$$

and

$$K_0 \left.\frac{\partial T_0}{\partial r}\right|_{r=r_0} = -\bar{h}(T_a - T_0) \text{ on } \mathscr{C}_0 \tag{50}$$

In terms of the dimensionless variables

$$R = r/r_0,\ \Theta = (T_0 - T_f)/(T_a - T_f) \tag{51}$$

the mixed boundary value problem for $\Theta(R, \theta)$ is

$$\frac{1}{R}\frac{\partial}{\partial R}\left(R\frac{\partial \Theta}{\partial R}\right) + \frac{1}{R^2}\frac{\partial^2 \Theta}{\partial \theta^2} = 0,\ R \le 1,\ \theta \in [0, 2\pi] \tag{52}$$

$$\Theta = 0 \text{ on } \mathscr{C}_1\text{: } R = 1,\ \tfrac{\pi}{2} < \theta < \tfrac{3\pi}{2} \tag{53}$$

$$\frac{\partial \Theta}{\partial R} = \mathrm{Bi}(1 - \Theta) \text{ on } \mathscr{C}_0\text{: } R = 1,\ 0 \le \theta \le \tfrac{\pi}{2},\ \tfrac{3\pi}{2} \le \theta \le 2\pi \tag{54}$$

Here the Biot number Bi is defined as

$$\mathrm{Bi} = \bar{h} r_0 / K_0, \tag{55}$$

where $K_0(\mathrm{W.m^{-1}\,K^{-1}})$ is the thermal conductivity of the conductor (see Figure 2). This Dirichlet–Neumann problem (see Sneddon 1966) cannot be solved analytically, but is readily solved numerically by finite-difference techniques. The required heat flux at the root is

$$Q_1 = -K_0 \int_{\mathscr{C}_1} \left.\frac{\partial T_0}{\partial r}\right|_{r=r_0} r_0 d\theta \tag{56}$$

$$= -K_0 (T_a - T_f) \int_{\pi/2}^{3\pi/2} \frac{\partial \Theta(1, \theta)}{\partial R} d\theta. \tag{57}$$

On application of the divergence theorem to the boundary-value problem (Equations 52–55), it follows that

$$Q_1 = \bar{h} r_0 (T_a - T_f) q_1, \tag{58}$$

where q_1 is defined as

$$q_1 \int_{\mathscr{C}_0} (1 - \Theta(1, \theta)) d\theta \tag{59}$$

q_1 is readily obtained by quadratures once the numerical solution for $\Theta(R, \theta)$ is available.

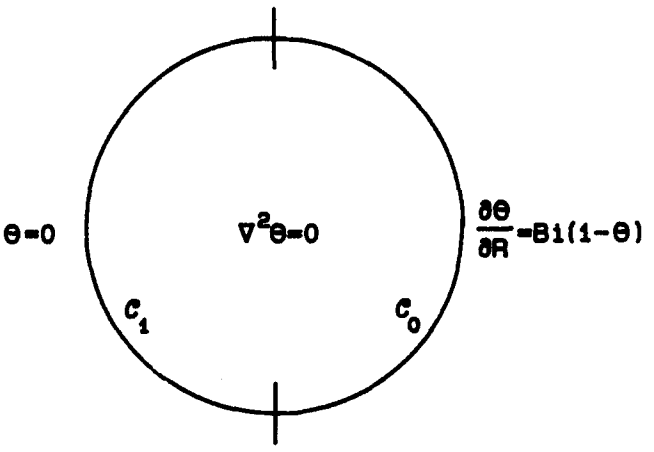

Figure 2 Mixed boundary value problem governing the steady-state temperature of the conductor

For the *noninsulated* conductor, the rate of production of melt water is given by a modified version of Equation 42, namely,

$$L_f \frac{dM_w}{dt} = (2\sigma G U t/\rho_s + \pi r_0) \times [\bar{h}(T_a - T_f) - \Lambda \chi_w \Delta e_w - (1 - \Lambda)\chi_i \Delta e_i] + \bar{h} r_0 (T_a - T_f) q_1 \tag{60}$$

and, consequently, the LWC is governed by the equation

$$\Lambda(T) = \gamma + \frac{1}{T}\int_0^T \left[\left(T + \frac{\pi}{2}\right)(\delta + \varepsilon\Lambda) + \alpha q_1\right] dT, \tag{61}$$

where

$$\alpha = \bar{h}(T_a - T_f)/(2\sigma G U L_f). \tag{62}$$

The solution of Equation 61 is given for the *noninsulated* case by Equation 46, with γ^* replaced by

$$\gamma^* = \gamma + \pi\delta/2 + \alpha q_1. \tag{63}$$

The above completes the formulation of the thermodynamic models for the prediction of LWC during the accretion modes of axial and cylindrical-sleeve growth. Some illustrative results are now given in the next section.

Results

Predictions of the LWC of the snow matrix, as a percentage of snow load, are presented graphically for the various thermodynamical models. In general, for constant climatological conditions, the values are taken as air temperature $T_a = 1°\mathrm{C}$, snow precipitation rate $P = 1.0$ mm $(H_2O).h^{-1}$, wind speed $U = 5\ \mathrm{m.s^{-1}}$, and relative humidity $\mathrm{Hr} = 0.95$. For snow accreting on a plane, the heat transfer coefficient is assumed to be $\bar{h} = 50\ \mathrm{W.m^{-2}\,K^{-1}}$; for snow accreting on a conductor of radius $r_0 = 1.863 \times 10^{-2}$ m, thermal conductivity $K_0 = 4\ \mathrm{W.m^{-1}\,K^{-1}}$, $\bar{h}$ depends on the Reynolds number of the conductor, as given by Equations 27 and 28. Table 1 lists the physical constants employed.

The LWC for the 1-D models is independent of time, so the following approach is adopted to highlight the dependence of LWC on the set of climatological parameters $\{T_a, P, U, \mathrm{Hr}\}$. Three of the parameters assume the constant values given above, while the fourth is allowed to vary, in turn, as

$$\left.\begin{aligned} T_a &= 2\eta \\ P &= 2\eta \\ U &= 10\eta \\ \mathrm{Hr} &= 0.9 + 0.1\eta \end{aligned}\right\} \text{ for } \eta \in (0, 1). \tag{64}$$

Figures 3a and 3b display the resulting four curves for the LWC of the plane snow layer when $\sigma = 1.0$ and when $\sigma = V_T/U$, respectively. The LWC at the point of intersection, which represents the LWC for the set of constant values {1.0, 1.0, 5,

Table 1 Physical properties of conductor and snow

Specific heat of air	c_a, J.kg.$^{-1}$ k^{-1}	1006
Kinematic viscosity of air	ν_a, m^2.s^{-1}	1.36×10^{-5}
Thermal conductivity of air	K_a, W.m^{-1}K^{-1}	2.42×10^{-2}
Thermal conductivity of conductor	K_0, W.m^{-1} K^{-1}	4.0
Latent heat of evaporation	L_E, J.kg^{-1}	2.51×10^6
Latent heat of fusion	L_f, J.kg^{-1}	3.25×10^5
Latent heat of sublimation	L_S, J.kg^{-1}	2.835×10^6
Radius of conductor	r_0, m	1.863×10^{-2}

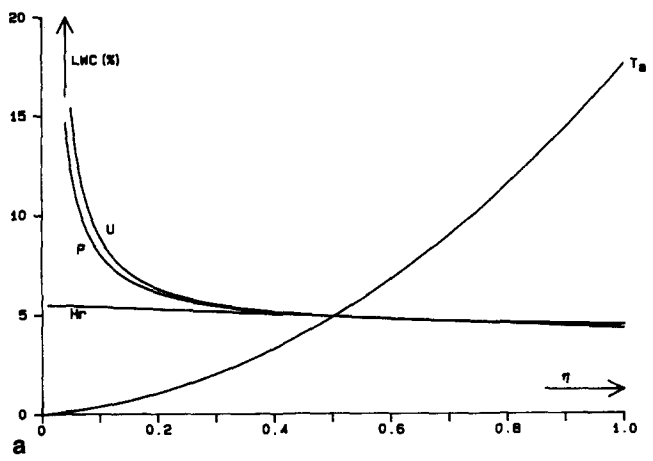

Figure 3a LWC as a function of air temperature, precipitation rate, wind speed, and relative humidity for the 1-D model: $\sigma = 1.0$

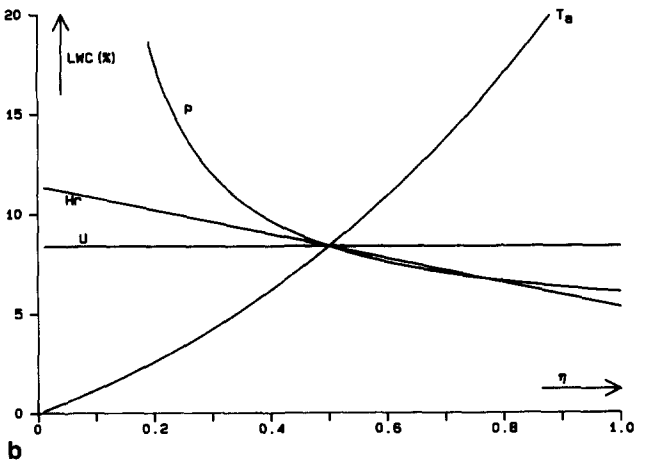

Figure 3b LWC as a function of air temperature, precipitation rate, wind speed, and relative humidity for the 1-D model: $\sigma = V_T/U$

0.95}, is about 5 percent for $\sigma = 1.0$ increasing to 8 percent for $\sigma = V_T/U$. Figure 3a shows that for $\sigma = 1.0$, the LWC increases rapidly with increasing T_a and decreases with increasing P, U, and Hr, especially for small values of P and U. Reducing the accretion factor σ to V_T/U (see Figure 3b) enhances the influence of the climatological parameters T_a, P, and Hr on the LWC, but the LWC is here independent of U, since σGU is constant. Many of these features may be seen more readily, for example, on rewriting Equation 24 for the plane layer in physical variables. Thus, for $\Delta T = (T_a - T_f) \in [0, 2]°C$,

$$\Lambda = \frac{\gamma + \bar{h}(T_a - T_f)(1 - \beta_1 \mathrm{Hr})/\sigma GUL_f}{1 - \bar{h}(T_a - T_f)\beta_2 \mathrm{Hr}/\sigma GUL_f}, \tag{65}$$

where

$$\beta_1 = 0.622 L_S/(c_a l^{2/3} H_0)\bar{e}_i \tag{66}$$

and

$$\beta_2 = 0.622(L_E \bar{e}_w - L_S \bar{e}_i)/(c_a l^{2/3} H_0) \tag{67}$$

and, from Lowe (1977), the vapor pressure–temperature coefficients are

$$\bar{e}_i = 0.0543 \text{ k.Pa.}°C^{-1} \tag{68}$$

$$\bar{e}_w = 0.0473 \text{ k.Pa.}°C^{-1}. \tag{69}$$

Corresponding graphs are shown in Figures 4a and 4b for the CSA model. The results are similar, except for $\sigma = V_T/U$, when LWC increases with increasing wind speed and the point of intersection is for the notably higher LWC of 23 percent.

The dependence on time of the LWC for the LRTA model is displayed in Figures 5a and 5b, for $\sigma = 1.0$ and $\sigma = V/U_T$, respectively. The results for the insulated conductor are compared with those for the noninsulated conductor over a period of 120 minutes. The LWC increases almost linearly with time, and the heat flux across the snow–conductor boundary $\mathscr{C}_1$ contributes to a considerably higher LWC than when the boundary is insulated. From Figure 5b it is clear that, for the noninsulated conductor, no accretion can occur for $\sigma = V_T/U$ when $T_a = 1.0°C$, since the LWC exceeds 80 percent; even when $T_a = 0.5°C$, the LWC is about 40 percent, as shown.

Conclusions

A theoretical investigation into the LWC of the snow deposit predicted by three simple thermodynamical models of snow accretion is presented. Analytical solutions are derived for LWC during wet-snow accretion on an insulated plane

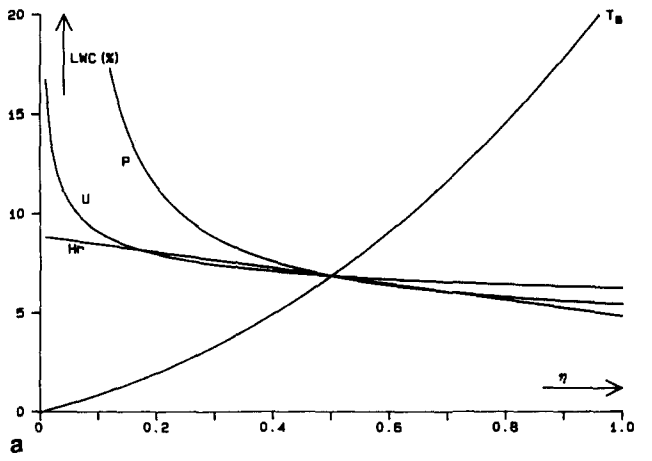

Figure 4a LWC as a function of air temperature, precipitation rate, wind speed, and relative humidity for the CSA model: $\sigma = 1.0$

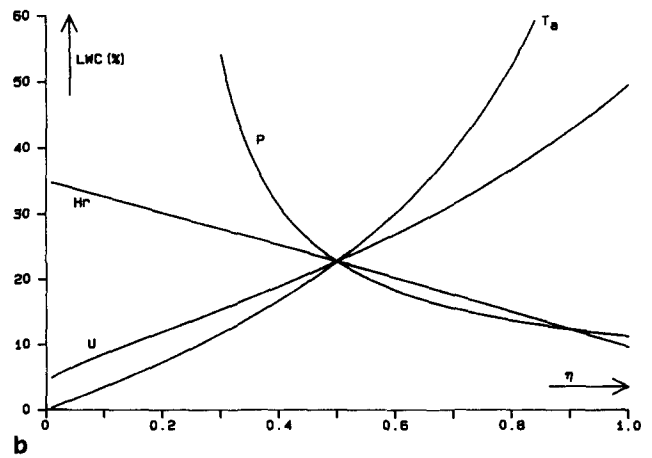

Figure 4b LWC as a function of air temperature, precipitation rate, wind speed, and relative humidity for the CSA model: $\sigma = V_T/U$

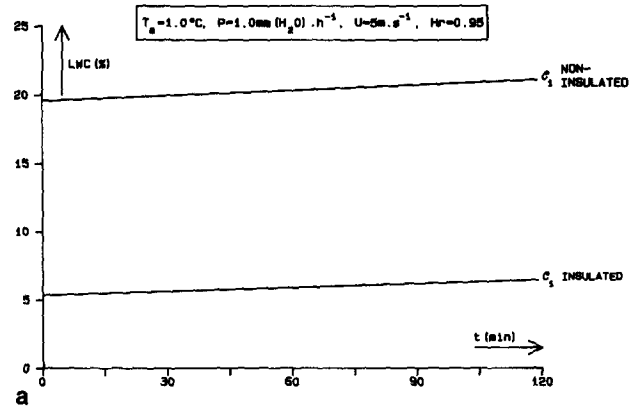

Figure 5a LWC of snow deposit for LRTA model: $\sigma = 1.0$

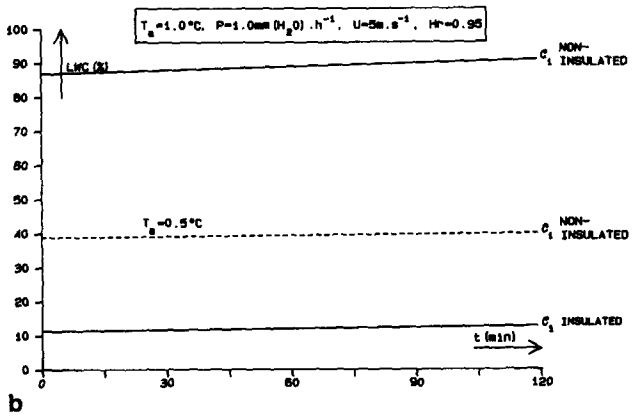

Figure 5b LWC of snow deposit for LRTA model: $\sigma = V_T/U$

surface, and for the accretion modes of axial and cylindrical-sleeve growth as occurs on a conductor span. For axial growth, a similar time-dependent solution is obtained whether the conductor is thermally insulated or not; in the latter case, the heat flux across the snow–conductor boundary is determined from the numerical solution of a mixed boundary value problem for the steady-state temperature of the conductor.

Acknowledgments

The authors are indebted to the National Grid Company for supporting this research, which is published by permission of the National Grid Company.

References

Admirat, P. and Sakamoto, Y. 1988. Wet snow on overhead lines: state-of-art. *Proc. Fourth Int. Conf. Atmospheric Icing of Structures*, Paris, 7–13

Admirat, P., Maccagnan, M., and De Goncourt, B. 1988a. Influence of Joule effect and of climatic conditions on liquid water content of snow accreted on conductors. *Proc. Fourth Int. Conf. Atmospheric Icing of Structures*, Paris, 367–370

Admirat, P., Sakamoto, Y., and De Goncourt, B. 1988b. Calibration of snow accumulation model based on actual cases in Japan and France. *Proc. Fourth Int. Conf. Atmospheric Icing of Structures*, Paris, 129–133

Chilton, T. J. and Colburn, A. P. 1934. Mass transfer coefficients. *Ind. Eng. Chem.*, **26**, 1183–1187

Grenier, J. C., Admirat, P., and Maccagnan, M. 1986. Theoretical study of the heat balance during the growth of wet-snow sleeves on electrical conductors. *Proc. Third Int. Conf. Atmospheric Icing of Structures*, Vancouver, 125–128

Lowe, P. R. 1977. An approximating polynomial for the computation of saturation vapour pressure. *J. Appl. Methods*, **16**, 100–103

Poots, G. and Rodgers, G. G. 1976. The icing of a cable. *J. Inst. Math. Appl.*, **18**, 203–217

Poots, G. and Skelton, P. L. I. 1992. A time-dependent heat and mass transfer model for icing of overhead transmission lines: Rime-ice and the onset of glaze. *Math. Eng. Ind.*, **3**, 265–283

Sakamoto, Y., Admirat, P., Lapeyre, J. L., and Maccagnan M. 1986. Modelling of wet snow accretion in a wind tunnel. *Proc. Third Int. Conf. Atmospheric Icing of Structures*, Vancouver, 67–71

Skelton, P. L. I. and Poots, G. 1991. Snow accretion on overhead line conductors of finite torsional stiffness. *Cold Reg. Sci. Technol.*, **19**, 301–316

Sneddon, I. N. 1966. *Mixed Boundary Value Problems in Potential Theory*. John Wiley and Sons, New York

Szilder, K., Waskiewicz, M., and Lozowski, E. P. 1988. Measurement of the average convective heat transfer coefficient and the drag coefficient for icing shaped cylinders. *Proc. Fourth Int. Conf. Atmospheric Icing of Structures*, Paris, 147–151

Wakahama, G., Kuroiwa, D., and Goto, K. 1977. Snow accretion on electric wires and its prevention. *J. Glaciol.*, **19**(8), 479–487